Show Me: Unifying Instructional Image and Video Generation with Diffusion Models

Yujiang Pu¹ Zhanbo Huang¹ Vishnu Boddeti¹ Yu Kong¹

¹Michigan State University

{puyujian, huang247, vishnu, yukong}@msu.edu

Abstract

Generating visual instructions in a given context is essential for developing interactive world simulators. While prior works address this problem through either text-guided image manipulation or video prediction, these tasks are typically treated in isolation. This separation reveals a fundamental issue: image manipulation methods overlook how actions unfold over time, while video prediction models often ignore the intended outcomes. To this end, we propose **ShowMe**, a unified framework that enables both tasks by selectively activating the spatial and temporal components of video diffusion models. In addition, we introduce structure and motion consistency rewards to improve structural fidelity and temporal coherence. Notably, this unification brings dual benefits: the spatial knowledge gained through video pretraining enhances contextual consistency and realism in non-rigid image edits, while the instructionguided manipulation stage equips the model with stronger goal-oriented reasoning for video prediction. Experiments on diverse benchmarks demonstrate that our method outperforms expert models in both instructional image and video generation, highlighting the strength of video diffusion models as a unified action-object state transformer. Our code will be available at https://yujiangpu20. github.io/showme/.

1. Introduction

Imagine you need to cook a steak or fold a shirt—what would you do? Most likely, you'd turn to a recipe or a YouTube video, reviewing it until you understand the steps. With the rise of large language models (LLMs) [1, 6, 57], you could even receive step-by-step instructions. However, while LLMs excel at generating detailed textual guidance, humans naturally interpret and learn through visual cues. YouTube videos, though visual, often present standardized procedures that may not align with a user's specific context. This highlights the need for generating visual instructions

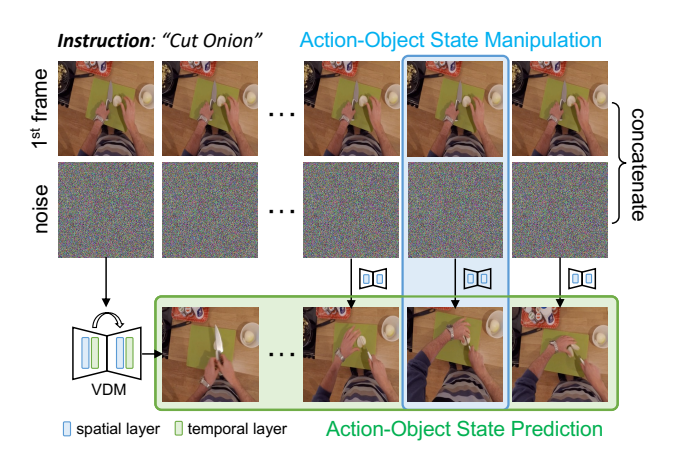


Figure 1. Video diffusion models inherently capture both spatial consistency and temporal dynamics, making them well-suited for unified action-object state transformations.

that are tailored to the user's situation, providing in-context, visually grounded guidance for complex tasks.

Despite its practical significance, visual instruction generation remains underexplored in the literature. LEGO [34] is the first work to generate instructional images of human actions from an egocentric view. It utilizes LLaVA [39] to produce enriched action descriptions, enabling diffusion models to achieve egocentric action manipulation. Concurrently, GenHowTo [54] collects action frames along with action-state captions from instructional videos, enabling action and object state transformations by fine-tuning Control-Net [71]. Later, StackDiffusion [43] generates illustrated instructions that meet user requirements by combining LLMs with text-to-image generation models. However, these efforts remain limited to creating "static" instructions that solely depict action execution or final object states.

To address this limitation, recent works have shifted toward instructional video generation. Seer [18] formulates the task as video prediction conditioned on an initial frame and a natural language instruction. Meanwhile, UniSim [69] builds a universal visual simulator by learning from diverse real-world and simulated data, enabling

the prediction of visual outcomes based on both high-level instructions and low-level actions. AID [66] further adapts the pretrained Stable Video Diffusion [3] model using lightweight adapters and leverages LLaVA to produce step-by-step guidance as additional textual conditions. However, these studies primarily focus on overall generation quality, while overlooking the semantic alignment and spatiotemporal consistency required by specific instructions.

Despite sharing the goal of modeling action-object transformations, instructional image and video generation are typically studied in isolation. We argue that this separation introduces a fundamental limitation: image manipulation methods are blind to how actions unfold over time, while video prediction models often fail to capture the intended outcomes. This disconnect raises a natural question: *Can a single model learn both to manipulate and to predict action-object transformations by sharing spatiotemporal priors?*

To this end, we propose **ShowMe**, a unified framework that enables both instructional image and video generation. Intuitively, we treat both tasks as two manifestations of action-object transformation, *i.e.*, state manipulation and state prediction. Our key insight is that pretrained video diffusion models (VDMs) inherently capture both spatial consistency and temporal dynamics. By decoupling the components and selectively tuning them via task-specific adapters, we demonstrate that a single VDM can be effectively repurposed to handle both tasks, as shown in Fig. 1.

Specifically, we realize this framework through a twostage tuning strategy. In the first stage, we disable the temporal modules of the VDM and fine-tune the spatial components using LoRA [27] for action-object state manipulation, further guided by structural rewards derived from depth and edge priors. In the second stage, we reactivate the temporal layers and train a separate set of LoRA adapters for state prediction, guided by a motion consistency reward to encourage smooth and coherent dynamics. Notably, the pretrained LoRA from the first stage is retained and frozen during this phase, equipping the model with strong spatial reasoning to support faithful action execution. This unification benefits both tasks: video pretraining provides contextual coherence for more realistic action-object state manipulation, while instruction-guided manipulation enhances video prediction by promoting goal-oriented outcomes.

In summary, our contributions are as follows:

- We propose ShowMe, a unified framework that repurposes VDMs as action-object state transformers, enabling both instructional image and video generation.
- We propose a two-stage tuning strategy with task-specific adapters while introducing structure and motion rewards to enhance spatial fidelity and temporal coherence.
- We demonstrate that ShowMe generalizes well across diverse image and video benchmarks, surpassing specialized baselines in both manipulation and prediction tasks.

2. Related Work

2.1. Diffusion-based Image Manipulation

Image manipulation has advanced significantly with the advent of diffusion models, enabling more intuitive and controllable editing of visual content. SDEdit [42] enables precise image synthesis by using stochastic differential equations to perturb and denoise images, leveraging the reverse process of diffusion models for guided manipulation. Later, Prompt-to-Prompt [20] achieves training-free editing by controlling cross-attention layers in pre-trained diffusion models, enabling localized and fine-grained edits through modifications to the input text prompt. InstructPix2Pix [5] further developed a large dataset of paired images and editing instructions, allowing models to accurately follow natural language commands for image editing without detailed prompts or masks. Despite these efforts, existing methods primarily focus on altering images' appearance, structure, or style, with little exploration of non-rigid edits related to human actions or object states. LEGO [34] first proposes to create detailed action descriptions through visual instruction tuning, which also integrates image and text embeddings from LLaVA [39] as additional conditions for egocentric action frame generation. Concurrently, GenHowTo [54] fine-tunes ControlNet [71] to learn action and object state transformations separately. A recent work, AURORA [33] explores the action and reasoning-centric image editing.

The work most related to ours is ShowHowTo [55], which also employs video diffusion models to generate contextually consistent step-by-step visual instructions. In contrast, we focus on state changes under single-step instructions and further extend this to video generation. Moreover, while ShowHowTo injects step-level instructions into frames through cross-attention, we adopt a spatio-temporal decoupling strategy to activate the editing capability and introduce reward tuning to improve structural fidelity. More quantitative and qualitative comparisons are presented in the following experiments.

2.2. Video Diffusion Models

Video diffusion models have garnered significant attention due to their potential in generating high-quality, temporally consistent frame sequences across various applications, including video editing [8, 9, 16, 75], interpolation [10, 14, 31, 40], and prediction [18, 26, 59, 68, 74]. VDM [25] is the first work extending 2D U-Net architectures to 3D spacetime with factorized attention for video generation. To reduce training costs, subsequent works [4, 19, 24, 51, 65] have focused on extending text-to-image (T2I) models to text-to-video (T2V) generation by introducing additional temporal modules, showing impressive performance. Another research direction is (text-)image-to-video (I2V) generation [3, 60, 64, 70, 73], which aims to produce coher-

ent video sequences based on conditional frames and text prompts. Additionally, some work has explored incorporating other control signals, such as pose [28, 41], structure [15, 63], and motion [29, 36, 50], as conditions to generate personalized videos that align with user preferences.

However, existing methods focus primarily on artistic creation or entertainment, leaving the conditional generation of human actions and object state changes underexplored. Seer [18] takes an early step by extending Stable Diffusion [49] for instruction-guided video prediction. UniSim [69] builds a world simulator using a VDM to learn interactive control and decision-making from large-scale internet data. More recently, AID [66] leverages LLaVA to generate detailed instructions and adapts SVD [3] for video prediction. In contrast, we curate instructional video datasets and introduce comprehensive benchmarks to evaluate both semantic alignment and spatiotemporal coherence, which are absent in these prior works.

3. Method

Preliminaries. Diffusion models [23, 53] are generative models that learn to produce data by simulating a gradual denoising process. Stable Diffusion [49] enhances this process by leveraging a variational autoencoder (VAE) [32] to encode images as latent variables, denoted as $\mathbf{z}_0 = \mathcal{E}(\mathbf{x}_0)$. The forward process $q(\mathbf{z}_t|\mathbf{z}_0,t)$, which gradually adds noise to \mathbf{z}_0 over T time steps, can be expressed as:

$$\mathbf{z}_t = \sqrt{\bar{\alpha}_t} \mathbf{z}_0 + \sqrt{1 - \bar{\alpha}_t} \epsilon, \epsilon \sim \mathcal{N}(\mathbf{0}, \mathbf{I}),$$
 (1)

where $\bar{\alpha}_t = \prod_{i=1}^t (1-\beta_t)$ controls the noise schedule. The reverse process is modeled as a learned Markov chain that approximates the posterior $p(\mathbf{z}_{t-1}|\mathbf{z}_t)$ to denoise the latent representation. To this end, the model learns a denoising function ϵ_{θ} to minimize the objective:

$$\mathcal{L} = \mathbb{E}_{\mathbf{z}_{0}, \mathbf{c}, \epsilon \sim \mathcal{N}(\mathbf{0}, \mathbf{I}), t} \left[\left\| \epsilon - \epsilon_{\theta}(\mathbf{z}_{t}, \mathbf{c}, t) \right\|_{2}^{2} \right],$$
 (2)

where \mathbf{c} indicates the condition that achieves controllable generation. During sampling, the reverse process starts from random Gaussian noise and iteratively denoises to generate the final latent variable $\hat{\mathbf{z}}_0$, which is then projected back to pixel space using the decoder, i.e., $\hat{\mathbf{x}}_0 = \mathcal{D}(\hat{\mathbf{z}}_0)$.

Problem Definition. In this work, we aim to tackle two closely related tasks: instructional image and video generation, both grounded in action-object transformations. Formally, given an initial image $\mathbf{x}^0 \in \mathbb{R}^{3 \times H \times W}$ and a textual instruction \mathbf{c} , our goal is to: (1) generate a target image $\hat{\mathbf{x}}^* \in \mathbb{R}^{3 \times H \times W}$ that reflects the execution of the instructed action with corresponding object state changes; and (2) generate a video $\hat{\mathbf{X}} = \{\hat{\mathbf{x}}^0, \dots, \hat{\mathbf{x}}^{L-1}\} \in \mathbb{R}^{L \times 3 \times H \times W}$ that illustrates the action's progression over time.

Framework Overview. We treat both tasks as two manifestations of action-object transformation, *i.e.*, state manipulation and state prediction, and address them within a

unified framework, as illustrated in Fig. 2. For state manipulation, we disable the temporal modules of the pretrained VDM and apply LoRA to the Q-Former and spatial layers, unlocking inherent state reasoning capabilities. We further introduce structure consistency rewards to enhance spatial perception and grounding. For state prediction, we activate the temporal modules and add separate LoRA adapters, followed by motion reward tuning to improve temporal coherence. By selectively activating the spatial or temporal LoRAs, our method seamlessly switches between instructional image and video generation during inference.

3.1. Action-Object State Manipulation

Human actions and object states evolve over time, making video generation models well-suited as action-state transformers operating along the temporal dimension. Inspired by this, we repurpose a pretrained video diffusion model, DynamiCrafter [64], for state manipulation.

The vanilla DynamiCrafter takes a reference image and a text prompt as conditions for video generation. To improve visual-text alignment, it extracts image embeddings using CLIP [46] and integrates them via a O-Former [35] projector. To adapt the model for action-object state manipulation, we first flatten it into a 2D U-Net by disabling the temporal modules, which allows the model to focus solely on spatial reasoning while ignoring temporal dynamics. We then insert LoRA [27] modules into the attention layers of both the Q-Former and the spatial transformer for efficient fine-tuning, as shown in Fig. 2. Since the initial and final frames of an instructional video naturally represent an object's starting and transformed states, respectively, we finetune the model with randomly sampled in-context video frame pairs $(\mathbf{x}^0, \mathbf{x}^*)$, supervised with the standard noise prediction objective defined in Eq. (2).

Although the fine-tuned model can manipulate images based on the action instruction, we observe that it often struggles to preserve the appearance and structure of the manipulated content. We argue that this issue arises from the model's limited ability to accurately perceive spatial relationships and locations within the 2D image context. To address this, we introduce a reward tuning strategy that incorporates two forms of structural information, i.e., depth and edge, to guide the generation process. Existing methods [11, 45, 67] mainly introduce the differentiable reward during the reverse process, resulting in significant time and computational costs. In contrast, we adopt a one-step approximation that enables efficient target image supervision during training. Moreover, our rewards focus on structure preservation by aligning with ground-truth geometry, whereas DRaFT [11] and AlignProp [45] primarily optimize for human preference alignment.

Specifically, we consider noisy latents from earlier diffusion steps t ($t \le \Gamma < T$) in the forward process as sam-

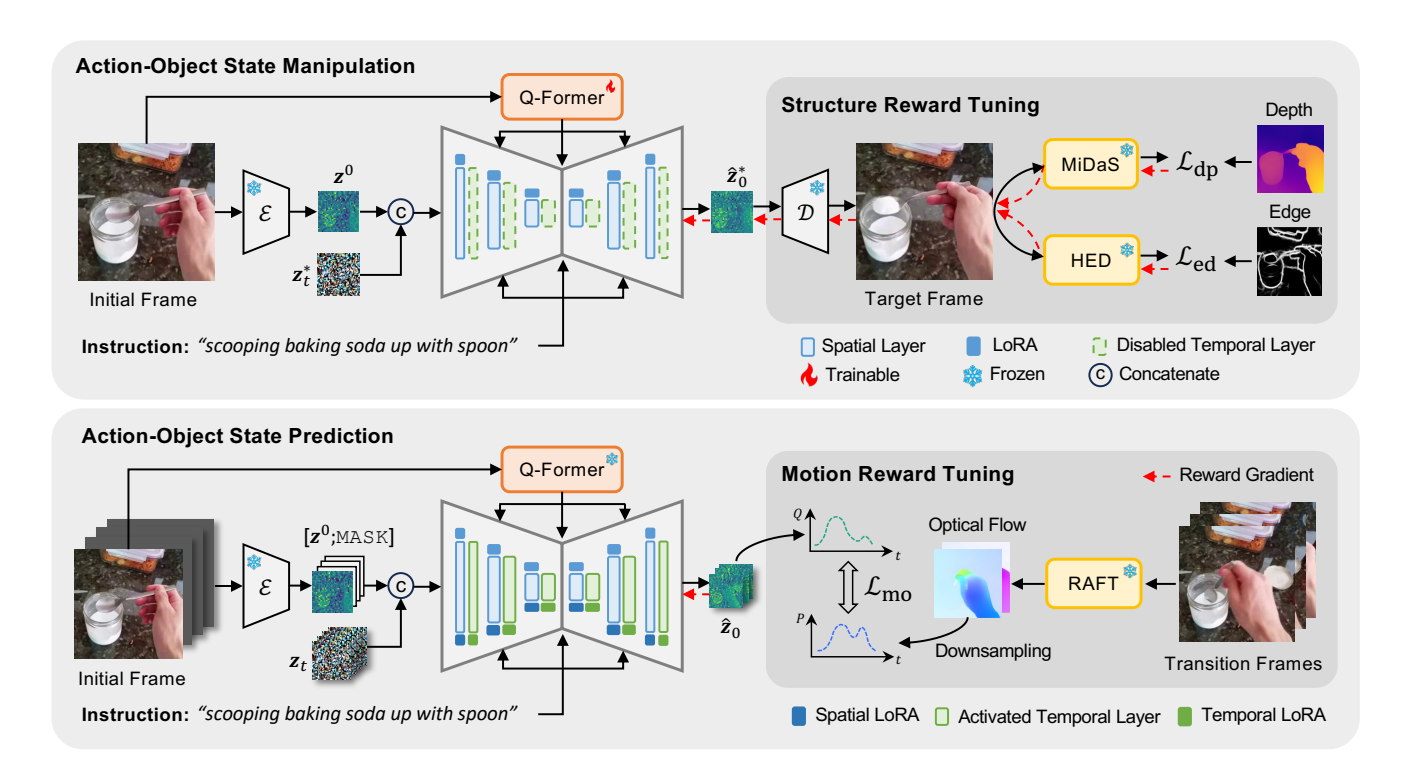


Figure 2. Illustration of the proposed **ShowMe** framework. For action-object state manipulation, we integrate LoRA into the Q-Former and spatial layers while disabling the temporal layers for model fine-tuning, followed by structure reward tuning to enhance depth and edge fidelity. For state prediction, we freeze all parameters and apply spatiotemporal LoRA for joint tuning, guided by motion reward to improve motion smoothness and consistency.

pling targets. As noted in [2, 23], such latents can be approximately denoised in a single step using the derivation from Eq. (1) and Eq. (2):

$$\mathbf{z}_{0}^{*} \approx \hat{\mathbf{z}}_{0}^{*} = \frac{\mathbf{z}_{t}^{*} - \sqrt{1 - \bar{\alpha}_{t}} \epsilon_{\theta}(\mathbf{z}_{t}^{*}, \mathbf{c}, t)}{\sqrt{\bar{\alpha}_{t}}},$$
 (3)

where $\hat{\mathbf{z}}_0^*$ is the estimated clean latent, which is then decoded into an RGB image via the VAE decoder \mathcal{D} . To introduce structural guidance, we leverage pretrained depth estimation [47] and edge detection [62] models. As shown in Fig. 2, the decoded image is passed through a depth estimator and an edge detector. Both reward models are frozen during fine-tuning. We then compute structural rewards \mathcal{L}_{dp} and \mathcal{L}_{ed} by measuring the mean squared error between the predictions and the corresponding ground-truth maps. The overall reward objective is defined as:

$$\mathcal{L}^* = \frac{1}{N} \sum_{i=1}^{N} \| \mathcal{R}_i(\mathcal{D}(\hat{\mathbf{z}}_0^*)) - \mathcal{R}_i(\mathbf{x}^*) \|_1, \qquad (4)$$

where \mathcal{R}_i refers to the *i*-th reward model (*e.g.*, depth or edge). By jointly optimizing this reward loss with the noise prediction objective, our method encourages structural fidelity and spatial coherence in the generated images. Qualitative improvements are illustrated in Fig. 5.

3.2. Action-Object State Prediction

By adapting the video diffusion model for instructional image generation, we equip it with enhanced visual grounding and object-state reasoning capabilities. Building on this foundation, the next challenge is to generate temporally coherent visual transitions from a given initial state, *i.e.*, to predict how an action unfolds over time.

The vanilla DynamiCrafter randomly samples video frames as conditions and concatenates them with repeated noisy latents to prevent positional shortcuts. In contrast, our task requires maintaining a fixed visual context to guide true prediction. Therefore, we fix the initial image at the starting position and apply zero padding as an unconditional mask, as shown in Fig. 2. We then activate the temporal modules and introduce a separate set of LoRA layers for spatiotemporal fine-tuning. Importantly, the pretrained LoRA modules from the manipulation stage are retained and frozen during this phase, providing strong spatial priors to support realistic state predictions.

However, we observe that this unconditional mask can result in abrupt and unrealistic motion patterns. To address this, we introduce a motion consistency reward to facilitate spatiotemporal coherence and smoothness. Intuitively, we can approximate clean latents via Eq. (3) and decode the full

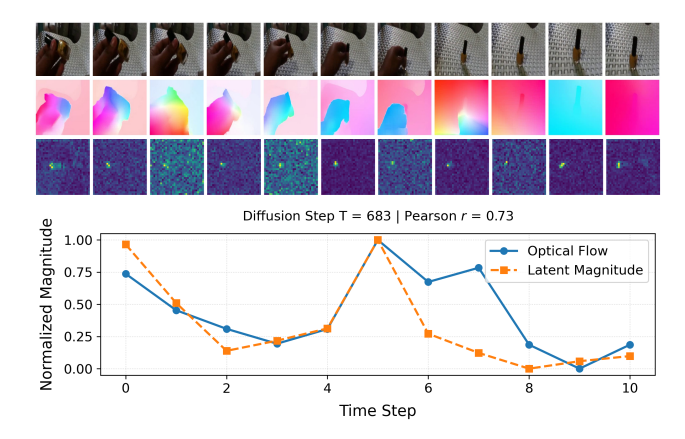


Figure 3. Motion consistency between flow and latent magnitude.

sequence back to pixel space for motion estimation. However, this inevitably incurs prohibitive memory and computational costs. A natural question arises: Can we apply motion rewards to the latent features without decoding them? We further visualize the ground-truth optical flow in pixel space alongside the temporal magnitude of one-step "denoised" latent features and observe that they exhibit strong temporal correlation, as shown in Fig. 3. Based on this observation, we propose to align the distribution of temporal magnitudes of latent features with the optical flow to improve motion smoothness and consistency.

Notably, unlike structural rewards that rely on low-level noisy samples, we find that motion information remains present even in highly noisy latents, as observed in [7]. Therefore, we perform one-step denoising on noisy latents from late diffusion steps using Eq. (3), and then compute the temporal magnitude of latent features as $\Delta \hat{\mathbf{z}}_i$ $\|\hat{\mathbf{z}}_{i+1} - \hat{\mathbf{z}}_i\|_2$. Meanwhile, we extract ground-truth optical flow using RAFT [56] and downsample it to match the latent resolution, denoted as $\{\hat{\mathbf{f}}_i\}_{i=1}^{L-1}$. We treat both the latent motion and pixel-space flow magnitude as temporal distributions at each spatial location. Specifically, we normalize the latent magnitude sequence and the downsampled flow magnitude sequence over the temporal dimension:

$$Q_{i}(h, w) = \frac{\Delta \hat{\mathbf{z}}_{i}(h, w)}{\sum_{j=1}^{L-1} \Delta \hat{\mathbf{z}}_{j}(h, w)},$$
 (5)

$$Q_{i}(h, w) = \frac{\Delta \hat{\mathbf{z}}_{i}(h, w)}{\sum_{j=1}^{L-1} \Delta \hat{\mathbf{z}}_{j}(h, w)},$$

$$P_{i}(h, w) = \frac{\hat{\mathbf{f}}_{i}(h, w)}{\sum_{j=1}^{L-1} \hat{\mathbf{f}}_{j}(h, w)}.$$
(6)

We then compute the Kullback-Leibler (KL) divergence of the two temporal distributions to obtain the motion reward:

$$\mathcal{L}_{\text{mo}} = \mathbb{E}_{h,w} \left[\text{KL}(P \parallel Q) \right]. \tag{7}$$

This objective encourages the model to follow realistic motion patterns, promoting smoother and more coherent predictions. Moreover, it eliminates the need to decode latents back to pixel space, allowing the model to process entire sequences and better preserve motion continuity.

4. Experiments

Datasets. We evaluate our method on two video datasets: Something-Something V2 [17] and Epic-Kitchens 100 [13]. SSv2 is a large dataset focusing on human interactions with everyday objects, consisting of 220,847 short video clips across 174 action categories, such as "picking up a pen" or "folding a shirt." We manually inspect the action labels and filter out static instructions like "holding" and "showing," as well as videos depicting "pretending to do" actions, resulting in 112,321 training samples and 2,048 test samples. Epic 100 captures daily kitchen activities from an egocentric perspective, comprising 100 hours of video footage with detailed narrations, including instructions such as "cut onion" and "stir vegetables." Similarly, we filter out videos featuring highly dynamic scenes or noticeable scene transitions, obtaining 57,602 training samples and 8,236 test samples. More details can be found in the supplementary material. **Evaluation Metrics.** For instructional image generation, we employ six metrics to evaluate the model's performance: CLIP-I [46] and DINO-I [44] for contextual consistency; CLIP-T for semantic alignment; Fréchet Inception Distance (FID) [21] for realism; Peak Signal-to-Noise Ratio (PSNR) and Learned Perceptual Image Patch Similarity (LPIPS) [72] for visual quality. For instructional video generation, we further incorporate Fréchet Video Distance (FVD) [58], VQAScore [38], and Motion Score [30]. VQAScore employs an MLLM to measure image-to-text alignment by computing the probability of a "Yes" answer to a question: <Image> Does this figure show {action instruction}? For Motion Score, we calculate Dynamic Degree and Motion Smoothness as proposed in VBench [30], and use their harmonic mean as the final metric. In addition, we utilize ViCLIP [61] and EgoVLP [37] to evaluate text-to-video alignment on SSv2 and Epic100, respectively.

4.1. Implementation Details

We implement ShowMe by adapting DynamiCrafter [64] through LoRA tuning in two stages. For action-object state manipulation, we first disable the temporal layers and freeze all pretrained parameters, training the LoRA within the projector and spatial transformers for 50K steps using a batch size of 256 and learning rate of 1e-4, followed by 20K steps with structure reward tuning. For action-object state prediction, we fine-tune another set of spatiotemporal LoRA for 20K steps using a batch size of 64 with motion consistency reward. Considering the computation cost, we uniformly sample 16 frames for Epic100 and 12 frames for SSv2, resizing to 256×256 resolution during both training and testing phases. During inference, we use the DDIM [52] sampler for 50 denoising steps and apply classifier-free guidance [22] with a ratio of 7.5 for text conditions. All experiments are conducted using 8 × RTX 6000 Ada GPUs.

Method		Sor	nething-Som	ething V	2		Epic-Kitchens 100					
	CLIP-I ↑	CLIP-T↑	DINO-I ↑	FID↓	PSNR ↑	LPIPS ↓	CLIP-I ↑	CLIP-T↑	DINO-I ↑	FID↓	PSNR ↑	LPIPS ↓
ControlNet [71]	0.8030	0.2870	0.5085	36.99	11.07	0.4590	0.8103	0.2532	0.5483	21.96	11.54	0.4866
SDEdit [42]	0.7809	0.2923	0.4249	34.60	13.30	0.4384	0.8115	0.2537	0.5373	16.00	12.65	0.4607
InstructPix2Pix [5]	0.8356	0.2902	0.5827	31.93	12.46	0.3868	0.8395	0.2562	0.6233	15.33	12.30	0.4358
GenHowTo [54]	0.8062	0.2813	0.5735	30.80	13.42	0.3921	0.8258	0.2528	0.6529	15.70	12.82	0.4293
AURORA [33]	0.8349	0.2894	0.5815	32.46	12.26	0.3927	0.8423	0.2569	0.6326	15.19	12.41	0.4314
ShowHowTo [55]	0.8428	0.2871	0.5875	31.32	11.23	0.4487	0.8539	0.2551	0.6290	14.18	12.54	0.4385
ShowMe (Ours)	0.8561	0.2860	0.6312	26.97	12.84	0.3778	0.8617	0.2462	0.6607	12.96	12.72	0.4232

Table 1. Performance of different image manipulation methods on instructional image generation. The compared methods are fully fine-tuned while our model only applies LoRA tuning. The best results are highlighted in **bold** and the second best is <u>underlined</u>.

Method	Something-Something V2			Epic-Kitchens 100								
111011101	FVD↓	FID↓	CLIP-I ↑	ViCLIP↑	VQA ↑	Motion ↑	FVD↓	FID↓	CLIP-I ↑	EgoVLP↑	VQA ↑	Motion ↑
AnimateAnything [12]	263.48	10.76	0.8752	0.1788	0.4704	10.19	263.59	5.04	0.8796	0.3198	0.5629	22.48
Seer [18]	144.55	18.10	0.8324	0.1865	0.4601	93.77	374.96	77.85	0.7491	0.2564	0.4821	91.03
ConsistI2V [48]	86.25	10.76	0.8479	0.1982	0.5093	90.30	90.45	10.20	0.8638	0.3535	0.5753	87.92
DynamiCrafter [64]	108.78	15.58	0.8193	0.1932	0.5108	90.77	119.29	15.00	0.8366	0.3343	0.5526	97.67
ShowMe (Ours)	74.66	10.21	<u>0.8584</u>	0.2012	0.5364	94.07	67.36	<u>9.01</u>	0.8637	0.3537	0.5815	<u>96.72</u>

Table 2. Performance of different I2V methods on instructional video generation. The compared methods are fully fine-tuned while our model only applies LoRA tuning. The best results are highlighted in **bold** and the second best is underlined.

4.2. Comparisons with State-of-the-Arts Methods

Instructional Image Generation. We first compare our method with state-of-the-art image manipulation models, including ControlNet [71], SDEdit [42], InstructPix2Pix [5], GenHowTo [54], AURORA [33] and ShowHowTo [55]. As shown in Tab. 1, ShowMe consistently outperforms competing methods in image-to-image metrics, achieving the highest CLIP-I and DINO-I scores and the lowest LPIPS on both datasets. This indicates that our model not only preserves semantic similarity but also maintains finer structural details. Notably, the compared methods are fully fine-tuned on these two datasets, while our model only applies LoRA tuning. We also notice that ShowMe has a lower CLIP-T score than all other methods. Interestingly, even ground-truth image-text pairs yield low CLIP-T scores (0.28 on SSv2 and 0.25 on Epic100), suggesting that CLIP-T may struggle to capture alignment between human actions and instructional images. This reveals a crucial limitation in previous methods: while they prioritize text similarity, they often sacrifice contextual fidelity, generating images that match the text superficially but fail to preserve scene consistency. We validate this finding with qualitative examples in Fig. 4, showing that while compared models produce semantically relevant images, they often alter key contextual elements, leading to discrepancies in action-object relationships. In contrast, ShowMe effectively balances semantic relevance with contextual consistency.

Instructional Video Generation. We further compare ShowMe with existing state-of-the-art I2V models, including AnimateAnything [12], Seer [18], ConsistI2V [48],

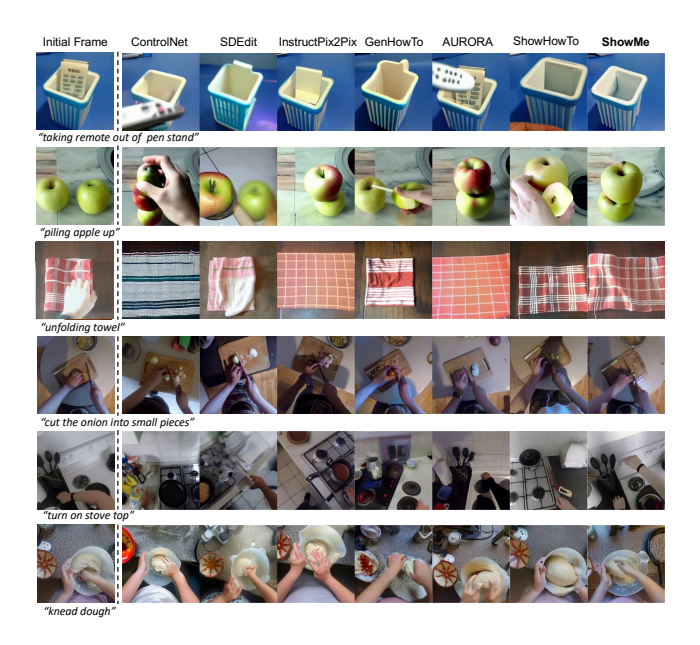
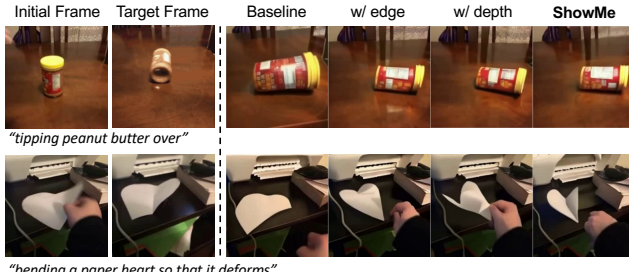


Figure 4. Comparison of different methods for instructional image generation. The first three rows are test samples from SSv2, and the last three rows are from Epic100. Our method is better at completing action instructions and maintaining contextual consistency.

and DynamiCrafter [64]. To ensure a fair comparison, we fully fine-tune all these methods on our curated datasets and report the final results. As shown in Tab. 2, ShowMe achieves consistently strong performance across both SSv2 and Epic100, notably delivering the lowest FVD scores on both datasets. While AnimateAnything achieves the high-



ending a paper heart so that it deforms

Figure 5. Visualization for the effect of structure reward tuning.

Method	CLIP-I ↑	CLIP-T↑	DINO-I ↑	FID ↓	PSNR ↑	LPIPS ↓
baseline	0.8434	0.2827	0.5967	29.84	12.01	0.4164
w/ $\mathcal{L}_{ ext{dp}}$	0.8532	0.2844	0.6255	28.25	12.56	0.3883
w/ $\mathcal{L}_{\mathrm{ed}}$	0.8553	0.2845	0.6299	26.92	12.77	0.3806
ShowMe	0.8561	0.2860	0.6312	26.97	12.84	0.3778

Table 3. Ablation of structure reward tuning on SSv2. 'baseline' means LoRA tuning without reward objectives.

Method	FVD↓	FID↓	CLIP-I ↑	$\text{ViCLIP} \uparrow$	$VQA \uparrow$	Motion ↑
ShowMe	74.66	10.21	0.8584	0.2012	0.5364	94.07
w/o \mathcal{L}_{mo}	86.74	11.00	0.8515	0.2003	0.5355	93.98
w/o Stage 1	110.73	12.54	0.8294	0.1971	0.5237	93.73

Table 4. Ablation of core components for instructional video generation on SSv2. 'Stage 1' means state manipulation.

est CLIP-I and the lowest FID, it exhibits the lowest Motion Score, indicating that it tends to generate nearly static frames, as evidenced in Fig. 7. Compared to Seer and DynamiCrafter, ShowMe maintains strong motion quality while excelling in semantic alignment (CLIP-T and VQA), demonstrating its ability to generate not only plausible movement but also accurate action-object interactions.

4.3. Ablation Studies

The effect of structure reward tuning. We report the ablation results of structure rewards in Tab. 3, showing that each reward contributes uniquely to improving generation quality. \mathcal{L}_{dp} enhances semantic alignment and perceptual quality, indicating that incorporating depth information helps preserve object structures. \mathcal{L}_{ed} further refines visual fidelity, leading to sharper details and better structural coherence. When combined, ShowMe achieves the best performance, demonstrating that depth and edge constraints complement each other, resulting in more faithful instructional images.

We further present qualitative results in Fig. 5 to highlight the impact of structural rewards. In the first row, the baseline model follows the instruction but fails to capture spatial relationships, resulting in incorrect object sizes and misaligned tag labels. Incorporating edge information preserves texture, while the depth reward improves understanding of rigid structures and 3D spatial layout. When both re-



Figure 6. Visualization for the effect of and motion reward tuning and 'Stage 1' (action-object state manipulation).

wards are combined, the edited image exhibits precise local edits with correct tag positioning and structural integrity.

The effect of components for instructional video generation. The ablation results in Tab. 4 further highlight the core contributions of ShowMe. Removing the motion consistency reward \mathcal{L}_{mo} results in degraded temporal coherence, as reflected in increased FVD and reduced CLIP-I and Motion scores. Notably, omitting Stage 1 leads to a substantial drop across all metrics, indicating its critical role in ensuring coherent spatial layouts and achieving the intended outcomes. Qualitative examples in Fig. 6 further illustrate these effects. Without motion rewards, the generated videos exhibit unnatural transitions, such as abrupt object movements during actions like package sliding. When Stage 1 is removed, the model fails to produce the correct final state, i.e., the package does not fall off the book, highlighting a loss in goal-directed reasoning. This supports our core claim: instruction-guided state manipulation not only enables meaningful edits but also strengthens video prediction by promoting goal-oriented visual outcomes.

4.4. Qualitative Analysis

Comparison of generated instructional videos. We further present a qualitative comparison with existing I2V generation models, as shown in Fig. 7. Our observations highlight key differences: (1) AnimateAnything often produces nearly "static" videos, exhibiting minimal human motion and failing to depict dynamic interactions; (2) Seer and ConsistI2V demonstrate some ability to follow instructions but struggle with maintaining visual coherence, either distorting the visual context or failing to preserve the structure of rigid objects; (3) ShowMe, in contrast, exhibits a stronger understanding of instructional prompts and executes them more faithfully. It not only captures clear human-object interactions, but also generates plausible state transformations, resulting in more realistic and contextually accurate video sequences. This highlights ShowMe's advantage in both semantic comprehension and visual consistency.



Figure 7. Generated instructional videos from different I2V models for two samples on SSv2 (left) and Epic100 (right).



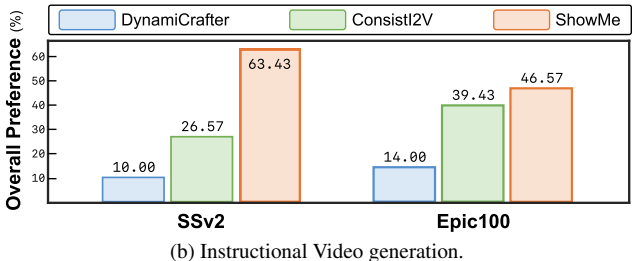


Figure 8. Human evaluation results. We conduct pairwise comparisons for instructional image generation and adopt a "winner-takes-all" setting for video generation.

Human Evaluation. Finally, we conduct a user study to evaluate the advantages of our method. We sample a subset of 50 examples for each dataset and collect the generated results from all baseline models. Each sample is evaluated by five Amazon Mechanical Turk workers, who are asked to select the candidate that best executes the instructed action while preserving the context of the original image. As shown in Figure 8a, ShowMe outperforms other models by a great margin on SSv2, achieving over 90% win rates against ControlNet and SDEdit, demonstrating its strengths

in contextual consistency and non-rigid editing. Notably, while ShowMe consistently outperforms other baselines on Epic100, the preference gap is smaller than that in SSv2. We argue that SSv2 involves diverse, nuanced daily-life actions requiring deeper reasoning, whereas Epic100's constrained kitchen scenarios present fewer challenges. This can be further supported by the video preference rate in Figure 8b, where ShowMe outperforms ConsistI2V by 36.86% on SSv2 and only 7.14% on Epic100.

Limitations. While our model can manipulate action object states, it struggles with complex edits from short instructions and with associating actions to non-salient objects correctly, sometimes producing objects "out of thin air" rather than manipulating existing ones. In addition, despite using structure reward tuning, the model may still struggle to distinguish the foreground in dynamic scenes, leading to object distortions and artifacts. Finally, our method currently generates only short clips rather than full videos, so extending it to long-term instructional tasks is a promising direction.

5. Conclusion

In this paper, we introduce ShowMe, a unified framework that reimagines diffusion models for both instructional image and video generation. We highlight the limitations of treating these tasks in isolation: image manipulation lacks temporal context, while video prediction often overlooks the intended outcome. ShowMe addresses these gaps by selectively activating spatial and temporal components and employing a two-stage tuning strategy with structure and motion rewards. Experiments show that ShowMe surpasses strong baselines, underscoring the potential of VDMs as a holistic solution for visual instruction generation.

Acknowledgements

This work was partially supported by the Office of Naval Research (ONR) grant (N00014-23-1-2417), and the Army Research Office (ARO) grant (W911NF-24-1-0385). Any opinions, findings, and conclusions or recommendations expressed in this material are those of the authors and do not necessarily reflect the views of ONR or ARO.

References

- [1] Josh Achiam, Steven Adler, Sandhini Agarwal, Lama Ahmad, Ilge Akkaya, Florencia Leoni Aleman, Diogo Almeida, Janko Altenschmidt, Sam Altman, Shyamal Anadkat, et al. Gpt-4 technical report. arXiv preprint arXiv:2303.08774, 2023. 1
- [2] Arpit Bansal, Hong-Min Chu, Avi Schwarzschild, Soumyadip Sengupta, Micah Goldblum, Jonas Geiping, and Tom Goldstein. Universal guidance for diffusion models. In Proceedings of the IEEE/CVF Conference on Computer Vision and Pattern Recognition, pages 843–852, 2023. 4
- [3] Andreas Blattmann, Tim Dockhorn, Sumith Kulal, Daniel Mendelevitch, Maciej Kilian, Dominik Lorenz, Yam Levi, Zion English, Vikram Voleti, Adam Letts, et al. Stable video diffusion: Scaling latent video diffusion models to large datasets. arXiv preprint arXiv:2311.15127, 2023. 2, 3
- [4] Andreas Blattmann, Robin Rombach, Huan Ling, Tim Dockhorn, Seung Wook Kim, Sanja Fidler, and Karsten Kreis. Align your latents: High-resolution video synthesis with latent diffusion models. In Proceedings of the IEEE/CVF Conference on Computer Vision and Pattern Recognition, pages 22563–22575, 2023. 2
- [5] Tim Brooks, Aleksander Holynski, and Alexei A Efros. Instructpix2pix: Learning to follow image editing instructions. In *Proceedings of the IEEE/CVF Conference on Computer Vision and Pattern Recognition*, pages 18392–18402, 2023. 2, 6
- [6] Tom B Brown. Language models are few-shot learners. arXiv preprint arXiv:2005.14165, 2020. 1
- [7] Ryan Burgert, Yuancheng Xu, Wenqi Xian, Oliver Pilarski, Pascal Clausen, Mingming He, Li Ma, Yitong Deng, Lingxiao Li, Mohsen Mousavi, et al. Go-with-the-flow: Motioncontrollable video diffusion models using real-time warped noise. In *Proceedings of the Computer Vision and Pattern* Recognition Conference, pages 13–23, 2025. 5
- [8] Duygu Ceylan, Chun-Hao P Huang, and Niloy J Mitra. Pix2video: Video editing using image diffusion. In *Proceedings of the IEEE/CVF International Conference on Computer Vision*, pages 23206–23217, 2023. 2
- [9] Wenhao Chai, Xun Guo, Gaoang Wang, and Yan Lu. Stable-video: Text-driven consistency-aware diffusion video editing. In *Proceedings of the IEEE/CVF International Conference on Computer Vision*, pages 23040–23050, 2023. 2
- [10] Xinyuan Chen, Yaohui Wang, Lingjun Zhang, Shaobin Zhuang, Xin Ma, Jiashuo Yu, Yali Wang, Dahua Lin, Yu Qiao, and Ziwei Liu. Seine: Short-to-long video diffusion model for generative transition and prediction. In *The*

- Twelfth International Conference on Learning Representations, 2023. 2
- [11] Kevin Clark, Paul Vicol, Kevin Swersky, and David J Fleet. Directly fine-tuning diffusion models on differentiable rewards. arXiv preprint arXiv:2309.17400, 2023. 3
- [12] Zuozhuo Dai, Zhenghao Zhang, Yao Yao, Bingxue Qiu, Siyu Zhu, Long Qin, and Weizhi Wang. Animateanything: Finegrained open domain image animation with motion guidance. arXiv preprint arXiv:2311.12886, 2023. 6
- [13] Dima Damen, Hazel Doughty, Giovanni Maria Farinella, Antonino Furnari, Evangelos Kazakos, Jian Ma, Davide Moltisanti, Jonathan Munro, Toby Perrett, Will Price, et al. Rescaling egocentric vision: Collection, pipeline and challenges for epic-kitchens-100. *International Journal of Computer Vision*, pages 1–23, 2022. 5
- [14] Duolikun Danier, Fan Zhang, and David Bull. Ldmvfi: Video frame interpolation with latent diffusion models. In *Proceedings of the AAAI Conference on Artificial Intelligence*, pages 1472–1480, 2024. 2
- [15] Patrick Esser, Johnathan Chiu, Parmida Atighehchian, Jonathan Granskog, and Anastasis Germanidis. Structure and content-guided video synthesis with diffusion models. In *Proceedings of the IEEE/CVF International Conference* on Computer Vision, pages 7346–7356, 2023. 3
- [16] Ruoyu Feng, Wenming Weng, Yanhui Wang, Yuhui Yuan, Jianmin Bao, Chong Luo, Zhibo Chen, and Baining Guo. Ccedit: Creative and controllable video editing via diffusion models. In *Proceedings of the IEEE/CVF Conference on Computer Vision and Pattern Recognition*, pages 6712–6722, 2024. 2
- [17] Raghav Goyal, Samira Ebrahimi Kahou, Vincent Michalski, Joanna Materzynska, Susanne Westphal, Heuna Kim, Valentin Haenel, Ingo Fruend, Peter Yianilos, Moritz Mueller-Freitag, et al. The" something something" video database for learning and evaluating visual common sense. In Proceedings of the IEEE international conference on computer vision, pages 5842–5850, 2017. 5
- [18] Xianfan Gu, Chuan Wen, Weirui Ye, Jiaming Song, and Yang Gao. Seer: Language instructed video prediction with latent diffusion models. *arXiv preprint arXiv:2303.14897*, 2023. 1, 2, 3, 6
- [19] Yuwei Guo, Ceyuan Yang, Anyi Rao, Zhengyang Liang, Yaohui Wang, Yu Qiao, Maneesh Agrawala, Dahua Lin, and Bo Dai. Animatediff: Animate your personalized text-to-image diffusion models without specific tuning. *arXiv* preprint arXiv:2307.04725, 2023. 2
- [20] Amir Hertz, Ron Mokady, Jay Tenenbaum, Kfir Aberman, Yael Pritch, and Daniel Cohen-Or. Prompt-to-prompt image editing with cross attention control. arXiv preprint arXiv:2208.01626, 2022. 2
- [21] Martin Heusel, Hubert Ramsauer, Thomas Unterthiner, Bernhard Nessler, and Sepp Hochreiter. Gans trained by a two time-scale update rule converge to a local nash equilibrium. Advances in neural information processing systems, 30, 2017. 5
- [22] Jonathan Ho and Tim Salimans. Classifier-free diffusion guidance. arXiv preprint arXiv:2207.12598, 2022. 5

- [23] Jonathan Ho, Ajay Jain, and Pieter Abbeel. Denoising diffusion probabilistic models. Advances in neural information processing systems, 33:6840–6851, 2020. 3, 4
- [24] Jonathan Ho, William Chan, Chitwan Saharia, Jay Whang, Ruiqi Gao, Alexey Gritsenko, Diederik P Kingma, Ben Poole, Mohammad Norouzi, David J Fleet, et al. Imagen video: High definition video generation with diffusion models. arXiv preprint arXiv:2210.02303, 2022. 2
- [25] Jonathan Ho, Tim Salimans, Alexey Gritsenko, William Chan, Mohammad Norouzi, and David J Fleet. Video diffusion models. *Advances in Neural Information Processing Systems*, 35:8633–8646, 2022. 2
- [26] Tobias Höppe, Arash Mehrjou, Stefan Bauer, Didrik Nielsen, and Andrea Dittadi. Diffusion models for video prediction and infilling. *arXiv preprint arXiv:2206.07696*, 2022. 2
- [27] Edward J Hu, Yelong Shen, Phillip Wallis, Zeyuan Allen-Zhu, Yuanzhi Li, Shean Wang, Lu Wang, and Weizhu Chen. Lora: Low-rank adaptation of large language models. *arXiv* preprint arXiv:2106.09685, 2021. 2, 3
- [28] Li Hu. Animate anyone: Consistent and controllable imageto-video synthesis for character animation. In *Proceedings of* the IEEE/CVF Conference on Computer Vision and Pattern Recognition, pages 8153–8163, 2024. 3
- [29] Zhihao Hu and Dong Xu. Videocontrolnet: A motion-guided video-to-video translation framework by using diffusion model with controlnet. arXiv preprint arXiv:2307.14073, 2023. 3
- [30] Ziqi Huang, Yinan He, Jiashuo Yu, Fan Zhang, Chenyang Si, Yuming Jiang, Yuanhan Zhang, Tianxing Wu, Qingyang Jin, Nattapol Chanpaisit, et al. Vbench: Comprehensive benchmark suite for video generative models. In *Proceedings of* the IEEE/CVF Conference on Computer Vision and Pattern Recognition, pages 21807–21818, 2024. 5
- [31] Siddhant Jain, Daniel Watson, Eric Tabellion, Ben Poole, Janne Kontkanen, et al. Video interpolation with diffusion models. In *Proceedings of the IEEE/CVF Conference* on Computer Vision and Pattern Recognition, pages 7341– 7351, 2024. 2
- [32] Diederik P Kingma. Auto-encoding variational bayes. arXiv preprint arXiv:1312.6114, 2013. 3
- [33] Benno Krojer, Dheeraj Vattikonda, Luis Lara, Varun Jampani, Eva Portelance, Chris Pal, and Siva Reddy. Learning action and reasoning-centric image editing from videos and simulation. Advances in Neural Information Processing Systems, 37:38035–38078, 2025. 2, 6
- [34] Bolin Lai, Xiaoliang Dai, Lawrence Chen, Guan Pang, James M Rehg, and Miao Liu. Lego: L earning ego centric action frame generation via visual instruction tuning. In *European Conference on Computer Vision*, pages 135–155. Springer, 2024. 1, 2
- [35] Junnan Li, Dongxu Li, Silvio Savarese, and Steven Hoi. Blip-2: Bootstrapping language-image pre-training with frozen image encoders and large language models. In *International conference on machine learning*, pages 19730–19742. PMLR, 2023. 3
- [36] Jingyun Liang, Yuchen Fan, Kai Zhang, Radu Timofte, Luc Van Gool, and Rakesh Ranjan. Movideo: Motion-aware

- video generation with diffusion model. In *European Conference on Computer Vision*, pages 56–74. Springer, 2025.
- [37] Kevin Qinghong Lin, Jinpeng Wang, Mattia Soldan, Michael Wray, Rui Yan, Eric Z Xu, Difei Gao, Rong-Cheng Tu, Wenzhe Zhao, Weijie Kong, et al. Egocentric video-language pretraining. Advances in Neural Information Processing Systems, 35:7575–7586, 2022. 5
- [38] Zhiqiu Lin, Deepak Pathak, Baiqi Li, Jiayao Li, Xide Xia, Graham Neubig, Pengchuan Zhang, and Deva Ramanan. Evaluating text-to-visual generation with image-to-text generation. In *European Conference on Computer Vision*, pages 366–384. Springer, 2024. 5
- [39] Haotian Liu, Chunyuan Li, Qingyang Wu, and Yong Jae Lee. Visual instruction tuning. *Advances in neural information processing systems*, 36, 2024. 1, 2
- [40] Haoyu Lu, Guoxing Yang, Nanyi Fei, Yuqi Huo, Zhiwu Lu, Ping Luo, and Mingyu Ding. Vdt: General-purpose video diffusion transformers via mask modeling. arXiv preprint arXiv:2305.13311, 2023. 2
- [41] Yue Ma, Yingqing He, Xiaodong Cun, Xintao Wang, Siran Chen, Xiu Li, and Qifeng Chen. Follow your pose: Poseguided text-to-video generation using pose-free videos. In *Proceedings of the AAAI Conference on Artificial Intelligence*, pages 4117–4125, 2024. 3
- [42] Chenlin Meng, Yutong He, Yang Song, Jiaming Song, Jiajun Wu, Jun-Yan Zhu, and Stefano Ermon. Sdedit: Guided image synthesis and editing with stochastic differential equations. *arXiv preprint arXiv:2108.01073*, 2021. 2, 6
- [43] Sachit Menon, Ishan Misra, and Rohit Girdhar. Generating illustrated instructions. In *CVPR*, pages 6274–6284, 2024. 1
- [44] Maxime Oquab, Timothée Darcet, Théo Moutakanni, Huy Vo, Marc Szafraniec, Vasil Khalidov, Pierre Fernandez, Daniel Haziza, Francisco Massa, Alaaeldin El-Nouby, et al. Dinov2: Learning robust visual features without supervision. arXiv preprint arXiv:2304.07193, 2023. 5
- [45] Mihir Prabhudesai, Anirudh Goyal, Deepak Pathak, and Katerina Fragkiadaki. Aligning text-to-image diffusion models with reward backpropagation. *arXiv preprint arXiv:2310.03739*, 2023. 3
- [46] Alec Radford, Jong Wook Kim, Chris Hallacy, Aditya Ramesh, Gabriel Goh, Sandhini Agarwal, Girish Sastry, Amanda Askell, Pamela Mishkin, Jack Clark, et al. Learning transferable visual models from natural language supervision. In *International conference on machine learning*, pages 8748–8763. PMLR, 2021. 3, 5
- [47] René Ranftl, Katrin Lasinger, David Hafner, Konrad Schindler, and Vladlen Koltun. Towards robust monocular depth estimation: Mixing datasets for zero-shot cross-dataset transfer. *IEEE transactions on pattern analysis and machine* intelligence, 44(3):1623–1637, 2020. 4
- [48] Weiming Ren, Huan Yang, Ge Zhang, Cong Wei, Xinrun Du, Wenhao Huang, and Wenhu Chen. Consisti2v: Enhancing visual consistency for image-to-video generation. arXiv preprint arXiv:2402.04324, 2024. 6
- [49] Robin Rombach, Andreas Blattmann, Dominik Lorenz, Patrick Esser, and Björn Ommer. High-resolution image

- synthesis with latent diffusion models. In *Proceedings of the IEEE/CVF conference on computer vision and pattern recognition*, pages 10684–10695, 2022. 3
- [50] Xiaoyu Shi, Zhaoyang Huang, Fu-Yun Wang, Weikang Bian, Dasong Li, Yi Zhang, Manyuan Zhang, Ka Chun Cheung, Simon See, Hongwei Qin, et al. Motion-i2v: Consistent and controllable image-to-video generation with explicit motion modeling. In ACM SIGGRAPH 2024 Conference Papers, pages 1–11, 2024. 3
- [51] Uriel Singer, Adam Polyak, Thomas Hayes, Xi Yin, Jie An, Songyang Zhang, Qiyuan Hu, Harry Yang, Oron Ashual, Oran Gafni, et al. Make-a-video: Text-to-video generation without text-video data. arXiv preprint arXiv:2209.14792, 2022. 2
- [52] Jiaming Song, Chenlin Meng, and Stefano Ermon. Denoising diffusion implicit models. *arXiv preprint arXiv:2010.02502*, 2020. 5
- [53] Yang Song, Jascha Sohl-Dickstein, Diederik P Kingma, Abhishek Kumar, Stefano Ermon, and Ben Poole. Score-based generative modeling through stochastic differential equations. arXiv preprint arXiv:2011.13456, 2020. 3
- [54] Tomáš Souček, Dima Damen, Michael Wray, Ivan Laptev, and Josef Sivic. Genhowto: Learning to generate actions and state transformations from instructional videos. In Proceedings of the IEEE/CVF Conference on Computer Vision and Pattern Recognition, pages 6561–6571, 2024. 1, 2, 6
- [55] Tomáš Souček, Prajwal Gatti, Michael Wray, Ivan Laptev, Dima Damen, and Josef Sivic. Showhowto: Generating scene-conditioned step-by-step visual instructions. In *Proceedings of the Computer Vision and Pattern Recognition Conference*, pages 27435–27445, 2025. 2, 6
- [56] Zachary Teed and Jia Deng. Raft: Recurrent all-pairs field transforms for optical flow. In Computer Vision–ECCV 2020: 16th European Conference, Glasgow, UK, August 23– 28, 2020, Proceedings, Part II 16, pages 402–419. Springer, 2020. 5
- [57] Hugo Touvron, Louis Martin, Kevin Stone, Peter Albert, Amjad Almahairi, Yasmine Babaei, Nikolay Bashlykov, Soumya Batra, Prajjwal Bhargava, Shruti Bhosale, et al. Llama 2: Open foundation and fine-tuned chat models. arXiv preprint arXiv:2307.09288, 2023. 1
- [58] Thomas Unterthiner, Sjoerd Van Steenkiste, Karol Kurach, Raphael Marinier, Marcin Michalski, and Sylvain Gelly. Towards accurate generative models of video: A new metric & challenges. arXiv preprint arXiv:1812.01717, 2018. 5
- [59] Vikram Voleti, Alexia Jolicoeur-Martineau, and Chris Pal. Mcvd-masked conditional video diffusion for prediction, generation, and interpolation. Advances in neural information processing systems, 35:23371–23385, 2022. 2
- [60] Xiang Wang, Hangjie Yuan, Shiwei Zhang, Dayou Chen, Jiuniu Wang, Yingya Zhang, Yujun Shen, Deli Zhao, and Jingren Zhou. Videocomposer: Compositional video synthesis with motion controllability. Advances in Neural Information Processing Systems, 36, 2024. 2
- [61] Yi Wang, Yinan He, Yizhuo Li, Kunchang Li, Jiashuo Yu, Xin Ma, Xinhao Li, Guo Chen, Xinyuan Chen, Yaohui Wang, et al. Internvid: A large-scale video-text dataset for

- multimodal understanding and generation. arXiv preprint arXiv:2307.06942, 2023. 5
- [62] Saining Xie and Zhuowen Tu. Holistically-nested edge detection. In CVPR, pages 1395–1403, 2015. 4
- [63] Jinbo Xing, Menghan Xia, Yuxin Liu, Yuechen Zhang, Yong Zhang, Yingqing He, Hanyuan Liu, Haoxin Chen, Xiaodong Cun, Xintao Wang, et al. Make-your-video: Customized video generation using textual and structural guidance. *IEEE Transactions on Visualization and Computer* Graphics, 2024. 3
- [64] Jinbo Xing, Menghan Xia, Yong Zhang, Haoxin Chen, Wangbo Yu, Hanyuan Liu, Gongye Liu, Xintao Wang, Ying Shan, and Tien-Tsin Wong. Dynamicrafter: Animating open-domain images with video diffusion priors. In European Conference on Computer Vision, pages 399–417. Springer, 2025. 2, 3, 5, 6
- [65] Zhen Xing, Qi Dai, Han Hu, Zuxuan Wu, and Yu-Gang Jiang. Simda: Simple diffusion adapter for efficient video generation. In Proceedings of the IEEE/CVF Conference on Computer Vision and Pattern Recognition, pages 7827– 7839, 2024. 2
- [66] Zhen Xing, Qi Dai, Zejia Weng, Zuxuan Wu, and Yu-Gang Jiang. Aid: Adapting image2video diffusion models for instruction-guided video prediction. arXiv preprint arXiv:2406.06465, 2024. 2, 3
- [67] Jiazheng Xu, Xiao Liu, Yuchen Wu, Yuxuan Tong, Qinkai Li, Ming Ding, Jie Tang, and Yuxiao Dong. Imagereward: Learning and evaluating human preferences for textto-image generation. Advances in Neural Information Processing Systems, 36, 2024. 3
- [68] Cheng Yan, Shiyu Zhang, Yang Liu, Guansong Pang, and Wenjun Wang. Feature prediction diffusion model for video anomaly detection. In *Proceedings of the IEEE/CVF International Conference on Computer Vision*, pages 5527–5537, 2023. 2
- [69] Mengjiao Yang, Yilun Du, Kamyar Ghasemipour, Jonathan Tompson, Dale Schuurmans, and Pieter Abbeel. Learning interactive real-world simulators. *arXiv preprint arXiv:2310.06114*, 2023. 1, 3
- [70] Yan Zeng, Guoqiang Wei, Jiani Zheng, Jiaxin Zou, Yang Wei, Yuchen Zhang, and Hang Li. Make pixels dance: High-dynamic video generation. In *Proceedings of the IEEE/CVF Conference on Computer Vision and Pattern Recognition*, pages 8850–8860, 2024. 2
- [71] Lvmin Zhang, Anyi Rao, and Maneesh Agrawala. Adding conditional control to text-to-image diffusion models. In Proceedings of the IEEE/CVF International Conference on Computer Vision, pages 3836–3847, 2023. 1, 2, 6
- [72] Richard Zhang, Phillip Isola, Alexei A Efros, Eli Shechtman, and Oliver Wang. The unreasonable effectiveness of deep features as a perceptual metric. In *Proceedings of the IEEE conference on computer vision and pattern recognition*, pages 586–595, 2018. 5
- [73] Shiwei Zhang, Jiayu Wang, Yingya Zhang, Kang Zhao, Hangjie Yuan, Zhiwu Qin, Xiang Wang, Deli Zhao, and Jingren Zhou. I2vgen-xl: High-quality image-to-video synthesis via cascaded diffusion models. *arXiv preprint arXiv:2311.04145*, 2023. 2

- [74] Zhicheng Zhang, Junyao Hu, Wentao Cheng, Danda Paudel, and Jufeng Yang. Extdm: Distribution extrapolation diffusion model for video prediction. In *Proceedings of the IEEE/CVF Conference on Computer Vision and Pattern Recognition*, pages 19310–19320, 2024. 2
- [75] Zicheng Zhang, Bonan Li, Xuecheng Nie, Congying Han, Tiande Guo, and Luoqi Liu. Towards consistent video editing with text-to-image diffusion models. Advances in Neural Information Processing Systems, 36, 2024. 2

Show Me: Unifying Instructional Image and Video Generation with Diffusion Models

Supplementary Material

A. Data Curation

A.1. Something-Something V2

The Something-Something v2 (SSv2) dataset is a comprehensive collection of labeled video clips illustrating human hand gestures and interactions with objects. It contains a diverse range of actions such as "Putting something into something," "Turning something," and "Pushing something from left to right." The original dataset comprises approximately 220,847 video clips, each around 4 seconds long, spanning 174 action categories. Compared to Epic100, SSv2 videos clearly exhibit an initial state and generally conclude with a frame depicting action completion. However, we identified several action categories without distinct human actions or meaningful object state changes, such as "holding," "showing," "fail," and "nothing happens," along with potentially harmful actions like "hitting" and "throwing." To ensure dataset relevance and safety, we manually reviewed all 174 action templates, identified and filtered out 62 categories containing keywords unlikely to reflect meaningful or useful changes. As a result, we curated the dataset to include 112,321 training samples and 2,048 test samples.

A.2. EPIC-KITCHENS 100

The EPIC-KITCHENS (Epic100) dataset comprises approximately 90,000 egocentric action segments with 20,000 unique narrations, covering 97 verb classes and 300 noun classes, recorded from daily kitchen activities. However, the continuous and unscripted nature of the recordings leads to challenges in generating coherent instructional videos. Specifically, egocentric videos often include highly dynamic actions and abrupt scene transitions, as shown in Fig. 9, and the end frames of narrations may not precisely align with the corresponding video clips. To address these challenges, we introduce a dual-similarity filtering approach to identify and remove videos with significant scene changes or misaligned content.

Our dual-similarity strategy involves two metrics:

- **Semantic Similarity**: We compute the similarity between text narrations and candidate frames using CLIP embeddings to ensure semantic alignment.
- **Visual Consistency**: We compute a framewise DINO similarity score between the initial frame and each of the downsampled last 8 frames.

By multiplying these two similarity scores, we measure the in-context semantic relevance and visual coherence of target frames. The frame with the highest combined sim-



Figure 9. Inconsistent visual context in egocentric instructional videos. From left to right: initial and target frames.

ilarity score is selected as the candidate target frame if its score exceeds a predefined threshold (We empirically set it to 0.1). Using this filtering strategy, we refined the dataset to 57,602 training samples and 8,236 test samples.

B. Ego4D Evaluation

To validate the effectiveness of our method, we followed LEGO's benchmark [34] setting and conducted additional experiments on Ego4D for instructional image generation. As shown in Table 5, our method achieves competitive results compared to LEGO. Importantly, LEGO fully finetunes Stable Diffusion with MLLM-enriched text instructions, whereas we only apply LoRA tuning with the vanilla action instructions provided in Ego4D. We further extend it for instructional video generation, where ShowMe consistently improves over the baseline and achieves the best FVD among all compared methods, as illustrated in Table 6.

Methods	EgoVLP↑	EgoVLP ⁺ ↑	CLIP-I↑	FID↓	PSNR ↑	LPIPS ↓	BLIP-B↑	BLIP-L↑
ProxEdit	44.51	72.68	68.17	33.01	11.88	40.90	17.73	17.35
SDEdit	50.07	72.90	73.35	33.35	11.81	41.60	19.80	19.74
IP2P	62.19	78.84	78.75	24.73	12.16	37.16	20.00	20.56
LEGO	65.65	80.44	80.61	23.83	12.29	36.43	20.38	20.70
ShowMe	66.93	79.14	79.77	19.38	11.92	35.59	19.76	22.28

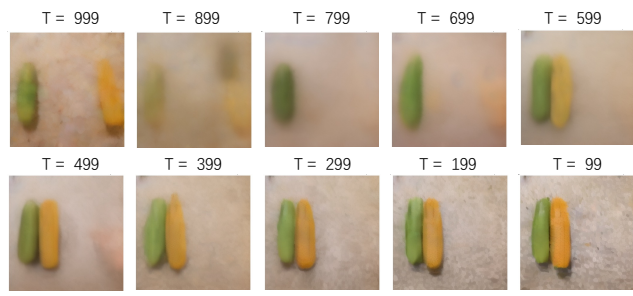
Table 5. Comparison of instructional image generation on Ego4D.

Methods	FVD↓	FID ↓	CLIP-I ↑	CLIP-T↑	EgoVLP↑	Motion ↑
AnimateAnything	271.14	13.24	0.8805	0.2541	0.3123	14.80
ConsistI2V	81.60	8.72	0.8768	0.2585	0.3628	74.61
DynamiCrafter	105.76	16.20	0.8401	0.2601	0.3064	96.69
ShowMe	72.51	12.00	0.8609	0.2613	0.3196	96.75

Table 6. Comparison of instructional video generation on Ego4D.

C. More Implementation Details

For action-object state manipulation and prediction, we set the LoRA rank to 128 and 64, respectively, with a dropout rate of 0.1. For structure reward tuning, we empirically set the diffusion threshold Γ for the one-step approximation to 200, and to 500 for motion reward tuning, as evidenced



Action Instruction: "moving corn and cucumber closer to each other"

Figure 10. Visualization of one-step denoising results at different diffusion steps.

in Fig. 10. The weights for \mathcal{L}_{dp} and \mathcal{L}_{ed} are both set to 1, while the weight for \mathcal{L}_{mo} is set to 0.001. During reward tuning, these loss functions work together with the noise prediction loss to optimize the model.

D. Reward Computation Cost

Table 7 shows that the dominant cost in Stage-1 is the gradenabled VAE decode, while the rewards themselves add only modest increments. In Stage-2, the motion reward operates entirely in latent space, incurring only a moderate computational cost. In practice, the observed training throughput reduction is acceptable given the gains in alignment and motion quality.

Stage	Component	ΔVRAM Peak	Time (ms)	ΔGFLOPs
Stage 1	VAE decode (grad) + Edge reward + Depth reward	+1.92 GB +0.19 GB +0.14 GB	187 368 1022	- 810 641
Stage 2	+ Motion reward	+0.79 GB	453	1559

Table 7. Complexity of reward tuning (per sample at 256², fp16).

E. Rationale for One-Step Approximation

We visualize one-step denoising samples at different diffusion steps during training, as shown in Fig. 10. It can be observed that at lower noise levels, the approximation closely resembles the target image and preserves spatial details well. In contrast, at higher noise levels (above 600), although structural information is lost, the approximated samples still capture the overall motion trends. This behavior aligns with the sampling process during inference: the model typically plans the global layout and motion patterns in the early high-noise steps, while refining spatial and structural details in the later denoising stages.

F. Limitations and Future Work

Finally, we present several failure cases in Figure 11 to illustrate the limitations of our method. In the first and third examples, when a scene contains multiple similar or complex

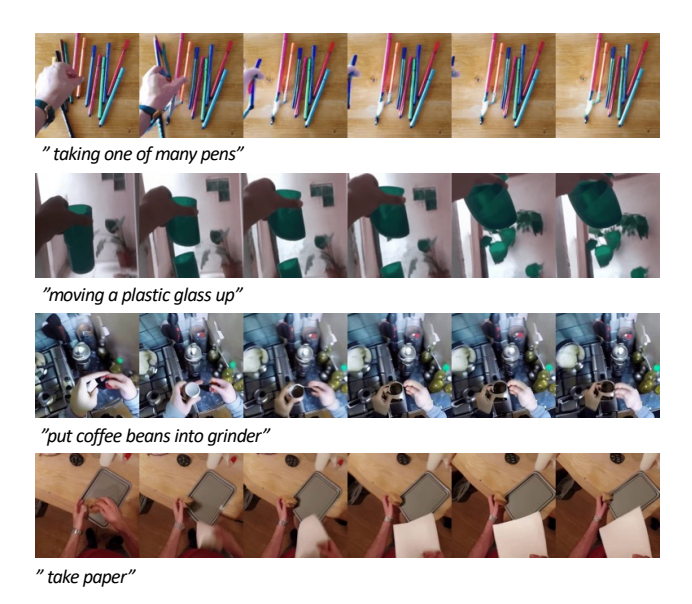


Figure 11. Failure examples. The first two rows are from SSv2 and the last two rows are from Epic100.

objects, the model struggles to ground the instruction precisely. For instance, distinguishing between "coffee beans" and the "grinder", which leads to task failure. In the second example, although the action is correct, the model's limited understanding of 3D space causes the plastic cup to appear split in half. In the final example, the model hallucinates a blank sheet of paper, indicating a failure to recognize the paper already being held. One possible solution is to introduce spatial grounding models for accurate target localization. In addition, explicitly conditioning on segmentation and depth information, along with using MLLMs to generate more detailed instructions, could further improve performance.

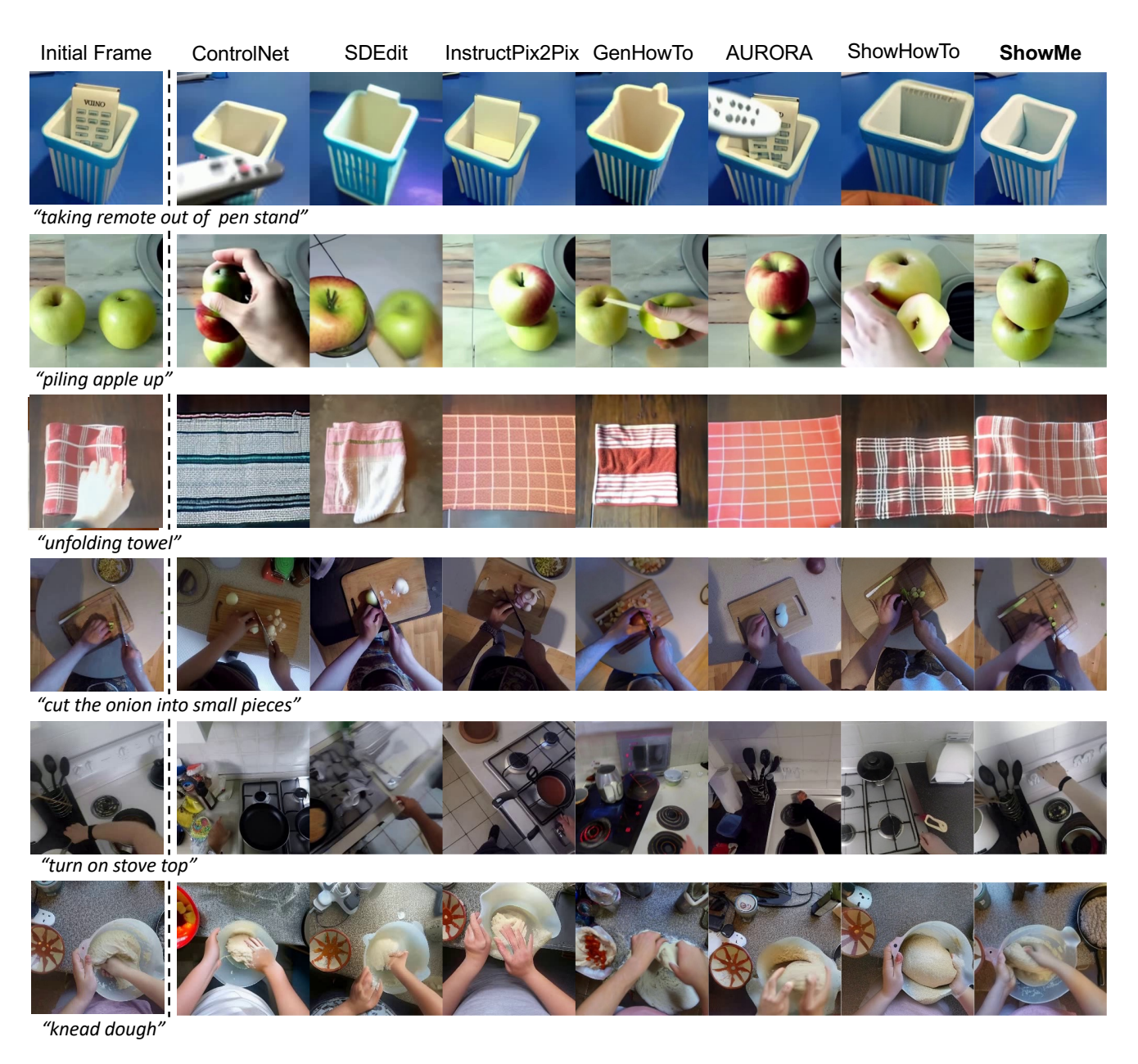


Figure 12. Comparison of different methods for instructional image generation. The first three rows are test samples from SSv2, and the last three rows are from Epic100. Our method is better at completing action instructions and maintaining contextual consistency.

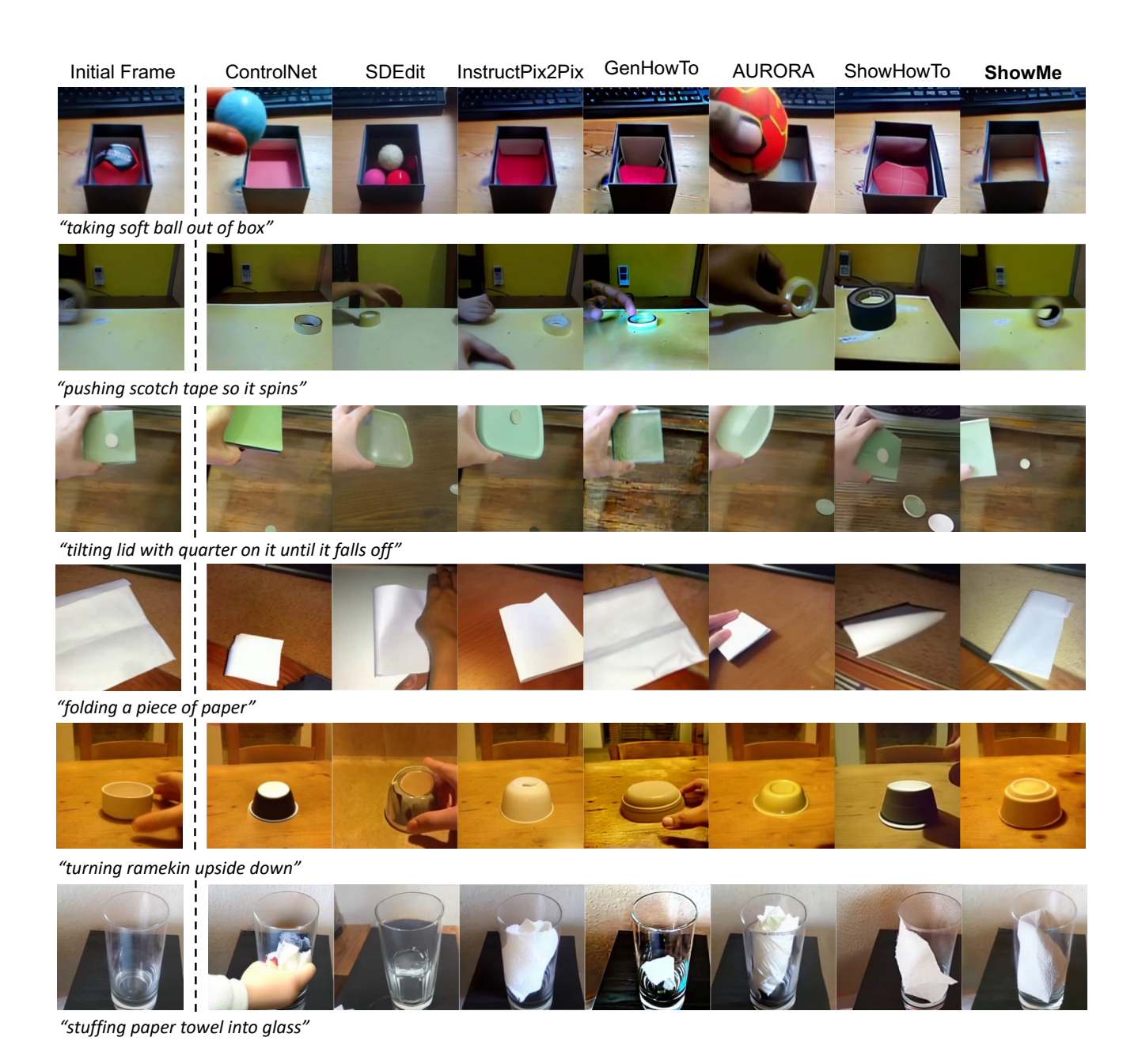
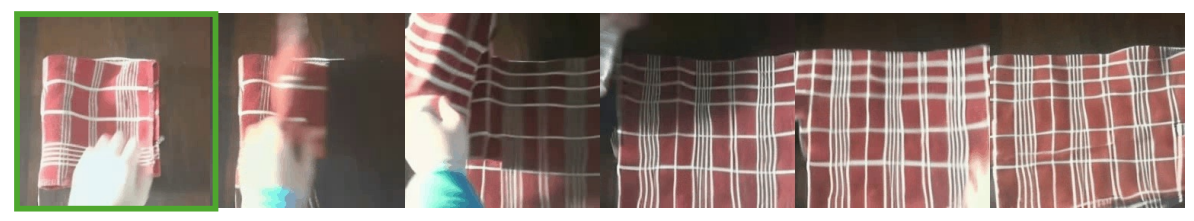


Figure 13. More visualization results of instructional image generation on SSv2.



"moving remote and small remote away from each other"



"unfolding towel"



"tearing paper"



"stuffing duvet into washing machine"



"poking tube so that it falls over"



"closing laptop"

Figure 14. Generated videos on SSv2 dataset.



"wash plate"



"open drawer"



"cut potatoes"



"rinse spoon"



"open fridge"



"stir food"

Figure 15. Generated videos on Epic100 dataset.